Journal of Applied Polymer Science

Low-Cost Upscaling Compatibility of Five Different ITO-Free Architectures for Polymer Solar Cells

Dechan Angmo,[1] Irene Gonzalez-Valls,[2] Sjoerd Veenstra,[3,6] Wiljan Verhees,[3,6] Subarna Sapkota,[4] Sebastian Schiefer,[4] Birger Zimmermann,[4] Yulia Galagan,[5,6] Jorgen Sweelssen,[5,6] Monica Lira-Cantu,[2] Ronn Andriessen,[5,6] Jan M. Kroon,[3,6] Frederik C. Krebs[1]

[1]Department of Energy Conversion and Storage, Technical University of Denmark, Frederiksborgvej 399, DK-4000 Roskilde, Denmark

[2]Centre de Investigaciò en Nanociencia i Nanotecnologia (CIN2-CSIC), Laboratory of Nanostructured Materials for Photovoltaic Energy, Campus UAB, Edifici ETSE 2nd Floor. Bellaterra (Barcelona), E-08193, Spain

[3]ECN, High Tech Campus 5, 5656 AE Eindhoven, The Netherlands

[4]Fraunhofer Institute for Solar Energy Systems ISE, Heidenhofstr. 2, 79110 Freiburg, Germany

[5]Holst Center, PO BOX 8550, 5605 KN Eindhoven, The Netherlands

[6]Solliance, High Tech Campus, 5656 AE Eindhoven, The Netherlands

Correspondence to: Frederik C. Krebs (E-mail: frkr@dtu.dk)

ABSTRACT: Five different indium-tin-oxide free (ITO-free) polymer solar cell architectures provided by four participating research institutions that all presented a laboratory cell performance sufficient for use in mobile and information and communication technology (ICT) were evaluated based on photovoltaic performance and lifetime tests according to the ISOS protocols. The comparison of the different device architectures was performed using the same active material (P3HT: PCBM) and tested against an ITO-based reference device. The active area was 1 cm^2 and rigid glass or flexible polyester substrates were employed. The performance results were corroborated by use of a round robin methodology between the four participating laboratories (DTU/DK, ECN/NL, Frauenhofer ISE/DE, and the Holst Centre/NL), while the lifetime testing experiments were carried out in only one location (DTU). Five different lifetime testing experiments were carried out for a minimum of 1000 h: (1) shelf life (according to ISOS-D-1); (2–3) stability under continuous 1 sun illumination (1000 Wm^{-2}, AM1.5G) at low (37 ± 3°C) and high (80 ± 5°C) temperatures (according to ISOS-L-1 and ISOS-L-2); (4) stability under continuous low-light conditions at 0.1 sun (100 Wm^{-2}, AM1.5G, 32°C) (according to ISOS-LL); (5) continuous illumination (670 Wm^{-2}, AM1.5G) at high temperature (65°C) and high humidity (50% RH) (according to ISOS-L-3). Finally, the upscaling compatibility of these device architectures based on the device photovoltaic behavior, stability and scalability were identified and we confirm that an architecture that presents a high score in only one aspect of the solar cell performance is not sufficient to justify an investment in upscaling. Many will require further technical development. © 2013 Wiley Periodicals, Inc. J. Appl. Polym. Sci. 130: 944–954, 2013

KEYWORDS: polymer solar cells, architectures, stability, upscaling, round robin and interlaboratory

Received 15 January 2013; accepted 15 February 2013; published online 17 April 2013
DOI: 10.1002/app.39200

INTRODUCTION

Polymer solar cells are an active research field where the main focus today is on improving the power conversion efficiency beyond 10%. This goal has recently been achieved through the use of very small active areas, delicate processing conditions, and exotic materials. Of significant interest is the possibility to develop these incarnations of the polymer solar cell into a useful technology that can be used to harvest energy on a meaningful scale for purposes beyond those of academic interest. The use of polymer solar cells as a power source for mobile and ICT applications such as mobile phones, PDAs, laptops, e-readers, e-labels, smart packaging, smart bandages, small lamps, etc. represent such a technological goal and the transformation of a laboratory solar cell into a technology suitable for mobile and ICT applications comprise several boundary conditions. First, the materials choice is limited and scarce or expensive materials such as indium cannot be employed. Second, the processing

Additional Supporting Information may be found in the online version of this article.

conditions that can practically be employed are likely to impose some limitations and the ultimate aim currently comprise ambient processing on flexible substrates using only benign solvents such as water. The use of inert conditions, clean-room or vacuum processing and use of rigid substrates such as glass have not been dismissed while it is likely that their use will imply that a given technology requiring these will be less competitive unless balanced by higher performance in some aspects (i.e., technical yield, performance, materials parsimony). Third, the active area of the device has to be scalable to 100 cm^2 or more to meaningfully enable supply of energy to mobile and ICT devices. Fourth, the operational stability of the device must be high enough to justify its use. Here, it is believed that the shelf life must exceed 5 years and the operational lifetime must be 2–3 years. Especially, the latter point represents a significant challenge as the service life required in the application is prohibitive for fast development unless accelerated and standardized lifetime measurements can be employed. It is also of significant interest to ensure that the results obtained are representative and corroborated between several laboratories such that reported values are based on a consensus average obtained between several independent or pseudo-independent operators.

In this report, we evaluate the photovoltaic properties and stability of five distinct ITO-free device structures. The ITO-free devices are provided by four participating institutions that have a rich experience in their respective device stack supplied to this study. As such, all devices compared in this work are optimized and can be regarded as the state-of-the art of their respective design. To enable comparison of the architectures, we have controlled the photoactive material (P3HT: PCBM) and the device area. In the absence of certification, a round robin study was carried out among the participating laboratories to corroborate device photovoltaic properties. An interlaboratory testing method was employed in the evaluation of stability under several accelerated lifetime testing conditions following protocols made in accordance with the ISOS consensus.[1] The ultimate aim of this article is to investigate each architecture from a photovoltaic property and stability point-of-view as well as to present a discussion on the implications of the respective choice of materials and processing of each architecture (given their photovoltaic and stability performance) on their suitability for low-cost upscaling.

EXPERIMENTAL

General Materials and Device Preparation

Five types of ITO-free device structures abbreviated as ALCR, AGNP, ASP, NORM, and WT were studied. An ITO-based inverted device was also included as reference. Table I lists materials, suppliers, deposition methods, and deposition conditions for all device architectures. Details on device fabrication can be found elsewhere: NORM,[2,3] ALCR,[4] AGNP,[5] and WT.[6] ASP devices utilizes a current collecting grid similar to that use in NORM and as described in Refs. 2 and 3 in an inverted architecture. ZnO is then spin coated to form the electron selective layer followed by spin coating of P3HT: PCBM (2 wt % in a 1 : 1 ratio in 1 mL of 1, 2-dichlorobenzene). PEDOT: PSS forms the hole transport layer and is overlaid by a metal grid electrode. It has been found crucial to deposit one layer (often ZnO) in the glove box and the device requires activation by application of a short pulse of high voltage (20 V) after processing. The WT is a wrap through device architecture known from inorganic solar cells[6] was redeveloped and adopted for flexible polymer solar cells. Reference ITO-based devices in inverted structure were fabricated with two different active area sizes: 0.36 and 1 cm^2. The ITO substrates were first thoroughly cleaned with ultrasonication in IPA and deionised water, and dried. The functional layers were then spin coated in the sequence: ZnO, P3HT: PCBM, and PEDOT: PSS consecutively. Reference devices of 1 cm^2 active area were based on P3HT: PCBM in 1: 1 (w/w) ratio in chlorobenzene with a total concentration of 60 mg mL^{-1} while 0.36 cm^2 devices were based on 1: 1 (w/w) ratio in 1,2-dichlorobenzene with a total concentration of 52 mg mL^{-1}. Both reference devices were completed with an evaporated Ag back electrode. Each reference devices were contributed by two institutions, and hence optimized differently.

Encapsulation Method

One method of encapsulation was adopted across all device structures to limit variability in stability due to barrier properties of the encapsulating material and the encapsulation method. The devices were encapsulated by sandwiching them between two glass slides (the substrate and encapsulation glass) using a UV curable DELO-ALP adhesive (LP655). The glue was homogeneously distributed by sliding two foldable clips with some force from the center of the device toward the edge. Finally, the device with the adhesive was exposed to UV radiation for a short time under a solar simulator (1 min with consequent heating to around 70°C) or under UV light to cure the adhesive.

Characterization

Round Robin. Round robin was carried out at four institutions: DTU (Denmark), ISE (Germany); Holst Centre (Netherlands), and ECN (Netherlands). All *IV* characterizations were done under 1000 Wm^{-2} at AM 1.5G solar irradiation. Prior to characterization, all devices were masked to achieve the desired aperture for accurate determination of the active area. At DTU, measurements were done under ambient conditions with the use of a sulfur plasma lamp with class A spectrum in the absorption range of the active material (it includes UV light). Prior to each measurement round, the light source was calibrated. Similar lamp sources were used at all other institutions except at Holst Center that employed an uncalibrated source. Mismatch factors based on the spectral response of all the devices were calculated under the standard solar spectrum and were found to be close to 1.

Interlaboratory Stability Tests. In this study, all devices were prepared by the individual participating institutions and sent to DTU where the experiments were initiated and data recorded for a period of up to 1000 h. Five different stability tests were carried out:

1. ISOS-D-1: Shelf life/Dark (25°C; 30 ± 5% RH).
2. ISOS-L-1: 1 sun (1000 W m^{-2}; AM 1.5G) at 37 ± 3°C.
3. ISOS-L-2: 1 sun (1000 W m^{-2}; AM 1.5G) at 80 ± 5°C.
4. ISOS-LL: Stability under indoor/low light conditions ~0.1 sun (100 W m^{-2}, AM 1.5G, 30°C, 10–15%RH)
5. ISOS-L-3: Stability under high temperature and humidity (0.67 sun, 65°C, 50% RH).

Table I. A Summary of the Device Architectures, Materials, Materials Suppliers, Deposition Methods, Substrates, and Deposition for the Devices Studied

Purpose	Device architectures	Materials	Material suppliers	Deposition method	Deposition conditions
Electrode 1 (electron contact)	ALCR NORM	Cr/Al/Cr	Sigma Aldrich	Evaporation	Vacuum
	ASP	Ag	Sun Chemical (Suntronic U5714)	Ink jet printed	Ambient
	AGNP		Hisense	Spin coated	
	Reference device	ITO	Lumtec/Naranjo substrate	As received/ sputter coated	Vacuum
Electron transport/ hole blocker	ALCR NORM	Cr LiF	Sigma Aldrich	Evaporation	Vacuum
	ASP	ZnO	In house prepared nanoparticles in IPA	Spin coating	N_2
	AGNP		In house prepared nanoparticles		Ambient
	Reference device				
Photoactive layer	ALCR NORM	P3HT: PCBM	Reike Metals Inc. 4002e	Spin coating	N_2
	ASP		Plextronics Plexcore OS2100: Solenne B.V.		Ambient
	AGNP				
	Reference device				
Hole transport/ electron blocker	ALCR	PEDOT: PSS	Clevios F010 and Agfa customized Formulation	Evaporation	N_2
	NORM			Spin coating	Ambient
	ASP		Agfa Orgacon EL-P 5015		
	AGNP		Agfa Orgacon EL-P 5010		
	Reference device		Agfa Orgacon EL-P 5010/5015		
Electrode 2 (Hole contact)	ALCR NORM	Au Al	Sigma Aldrich	Evaporation	Vacuum
	ASP	Ag	Toyo Rexalpha RA FS FD 018 (paste)	Screen printed	Ambient
	AGNP		Sigma Aldrich	Evaporation	Vacuum
	Reference device				
Substrate	ALCR NORM ASP	Glass	–		
	AGNP	PET	Melinex PET		
	Reference device	Glass	–		

Devices were stored in the dark (drawer) for ISOS-D-1 and in a climate chamber (QSun) for the ISOS-L-3 tests. These devices were intermittently measured for their photovoltaic properties by removing them from their test systems (drawer and the climate chamber) and measuring under a solar simulator at 1000 W m^{-2} (AM1.5G) after a brief (5 min) equilibration time. After the measurements, these modules were promptly returned back to their test systems. Devices were exposed to constant illumination under a solar simulator equipped with a metal halide lamp having a class B spectrum for ISOS-L-1 and L-2 tests. The temperature for ISOS-L-1 was controlled using a cooling system (fans) while the temperature was not actively controlled for ISOS-L-2 and represent the equilibrium temperature reached under the solar simulator (~80°C). The ISOS-LL test was conducted by keeping the devices under low light illumination provided by fluorescent tube lamps throughout the duration of the study. A custom built software recorded *IV*-properties every 15 min during the experiments for ISOS-L-1/-2 and ISOS-LL and no manual handling were involved. All experiments were carried out under calibrated light sources.

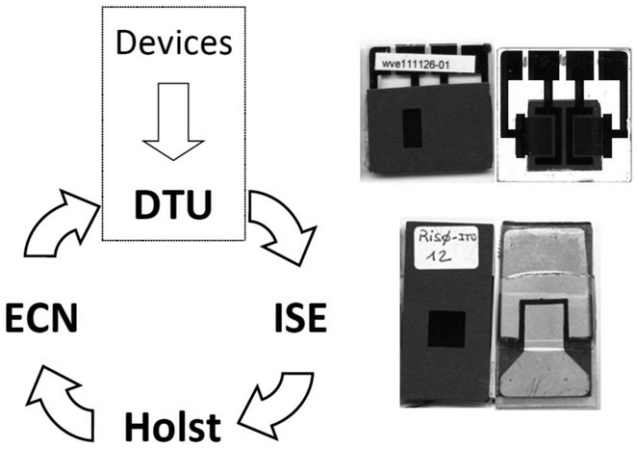

Figure 1. The round robin procedure is shown schematically on the left. Devices were prepared in four different institutions and sent to DTU for the first measurement. The devices were then sent around together according to the flow and tested at each location and finally tested again at DTU upon completion of the cycle. The rectangle indicates the long-term stability measurements where devices were prepared in any given number of institutions and sent to DTU for the degradation testing.

RESULTS AND DISCUSSION

Our approach was divided into four parts and accordingly the results are presented. In the first part, a round robin of reference devices (ITO-based) was carried out to corroborate the capacity of the participating laboratories with respect to determination of device photovoltaic performance. This was achieved through a round robin on ITO-based reference devices following a procedure shown in Figure 1. The agreement was found good enough to enable studies on new ITO-free device architectures. In the second part, a round robin of devices based on the five ITO-free architectures was carried out to evaluate their photovoltaic performance. Such a thorough examination of photovoltaic properties was carried out because measurement conditions of every laboratory are not identical even if calibrated light sources are used. Temperature under the solar simulator; and variables related to the light sources such as diffusivity, spectral- and temporal- responses may contribute to variations in reported efficiency.[7] Given the several independent laboratories involved in this study, it was essential to establish credibility of the reported power conversion efficiency (PCE) values. A round robin study provides a facile route to gain consensus on device performance in the absence of certification. In the third part, an interlaboratory stability evaluation of the devices based on the ITO-free architectures was carried out following several ISOS protocols. Finally, in the fourth part, we present an evaluation on the upscaling compatibility and potential of the presented ITO-free structures based on their respective photovoltaic properties, stability, and materials and processing requirements.

The Reference Device Round-Robin Evaluation

The round robin study of reference devices were carried out according to the procedure shown in Figure 1 on small and larger area devices and the results are summarized in Table II. The deviation in power conversion efficiency (PCE) is mainly contributed by the largest deviation in short circuit current density (J_{sc}) which has the maximum standard error between 9 and 11% for all reference devices. Open circuit voltage (V_{oc}) and fill factor (FF) have significantly lower spread with maximum error between 2 and 5% respectively among all four devices. While J_{sc} could vary to some extent because of degradation over the course of round robin (25 days), other factors such as the light sources and their calibration, operator's handling, and so forth, may all contribute to this variability. Both of the two devices with an active area of 0.36 cm^2 have higher than theoretically expected values of J_{sc} in both DTU-1 and DTU-5 measurements. We suspect that it is caused by an interplay of small

Table II. Results from the Round Robin Experiment on ITO-Based Reference Devices

Device area	0.36 cm^2				1 cm^2			
Laboratory	J_{sc} (mA cm^{-2})	V_{oc} (V)	FF (%)	PCE (%)	J_{sc} (mA cm^{-2})	V_{oc} (V)	FF (%)	PCE (%)
DTU-1	12.32	0.53	56	3.66	8.09	0.55	41	1.84
	12.85	0.51	58	3.82	8.47	0.55	40	1.86
ISE-2	9.71	0.5	56	2.75	8.21	0.54	41	1.82
	10.3	0.51	57	2.99	8.49	0.54	40	1.83
Holst-3	9.82	0.5	60	2.94	6.61	0.53	45	1.58
	10.27	0.5	59	3.04	6.91	0.53	45	1.65
ECN-4	9.89	0.51	60	3.01	7.94	0.54	42	1.8
	10.63	0.51	59	3.19	6.74	0.55	42	1.56
DTU-5	11	0.51	59	3.05	8.49	0.54	43	1.95
	11.53	0.52	57	3.11	7.04	0.54	42	1.59
Average	10.54 ± 1.11	0.51 ± 0.01	58.2 ± 2.05	3.08 ± 0.34	7.86 ± 0.73	0.54 ± 0.01	42.4 ± 1.67	1.80 ± 0.13
	11.11 ± 1.09	0.51 ± 0.007	58.0 ± 1.00	3.23 ± 0.34	7.53 ± 0.87	0.54 ± 0.01	41.8 ± 2.04	1.69 ± 0.15

The devices were prepared at ECN and DTU on glass substrates with active areas of 0.36 cm^2 and 1 cm^2, respectively. The measurements were carried out on two devices. The order listed (1–5) is the order in which the devices first were shipped across the participating laboratory for the round robin study.

Table III. Results from the Round Robin Experiment on the ITO-Free Device Architectures

Laboratory	J_{sc} (mA cm^{-2})	V_{oc} (V)	FF (%)	PCE (%)
NORM	6.27 ± 0.64 (10.23)	0.53 ± 0.01 (1.04)	61.60 ± 0.55 (0.89)	2.03 ± 0.22 (10.33)
	6.90 ± 0.64 (9.29)	0.52 ± 0.01 (1.36)	56.20 ± 0.45 (0.80)	2.01 ± 0.21 (10.81)
ASP	5.79 ± 0.55 (9.57	0.52 ± 0.01 (1.36)	52.40 ± 1.14 (2.18)	1.58 ± 0.1 (10.55)
	5.69 ± 0.58 (10.23)	0.53 ± 0.01 (1.70)	54.40 ± 3.05 (5.61)	1.58 ± 0.14 (9.10)
AGNP	3.27 ± 0.22 (6.72)	0.49 ± 0.01 (1.81)	56.20 ± 3.63 (6.46)	0.91 ± 0.09 (9.83)
	3.68 ± 0.21 (5.70)	0.54 ± 0.01 (1.02)	56.80 ± 0.45 (0.79)	1.12 ± 0.07 (5.91)
ALCR	7.06 ± 0.51 (7.18)	0.59 ± 0.01 (0.93)	61.80 ± 1.10 (1.77)	2.56 ± 0.16 (6.28)
	6.74 ± 0.36 (5.32)	0.58 ± 0.01 (0.95)	61.20 ± 0.84 (1.37)	2.37 ± 0.12 (4.85)
WT	5.53 ± 0.88 (15.90)	0.57 ± 0.02 (3.34)	32.50 ± 6.35 (19.54)	1.02 ± 0.32 (31.58)
	5.89 ± 1.27 (21.59)	0.57 ± 0.02 (2.64)	35.50 ± 2.38 (6.71)	1.19 ± 0.27 (22.58)

The measurements were carried out on two devices. All devices had an active area of 1 cm^2 except for the wrap-through (WT) devices with an active area of 2.25 cm^2. The data is the average taken from the round robin measurements and are reported in duplicate for the two devices. Given in parenthesis is the standard error in % (percentage of standard deviation to the average value). The detail round robin data is available in supporting information.

aperture area, thickness of the mask, the uniformity of the light under the solar simulator, the diffuse content of the light from the lamp of the solar simulator—all of which may result in the overestimation of photocurrent.[8] As a result of this uncertainty with small active area, an active area of 1 cm^2 was selected for efficiency and stability evaluation of ITO-free devices. As the standard error in all photovoltaic properties were lower than 10% (J_{sc}: 9%, V_{oc}: 2%; FF: 3.5%; PCE: 9%), the evaluation of photovoltaic properties of the ITO-free devices were carried out expecting similar standard error. Note that such a standard error is significantly lower than those reported in other round robin studies on polymer solar cells.[7,9]

Round-Robin of ITO-Free Architectures

Five different ITO-free device architectures were subjected to the same round robin procedure following the route presented in Figure 1. The ITO-free device outlines are shown in Figure 2 and their corresponding PCE can be visualized in Figure 3.

Despite the use of a common photoactive material (P3HT:PCBM) and the similar active area (1 cm^2), a large difference in the PCE among the various architectures is noticed. Table III summarizes the average of the key photovoltaic parameters of all ITO-free architectures based on the round robin data. The complete round robin data of all ITO-free architectures could be found in the Supporting Information. The difference in

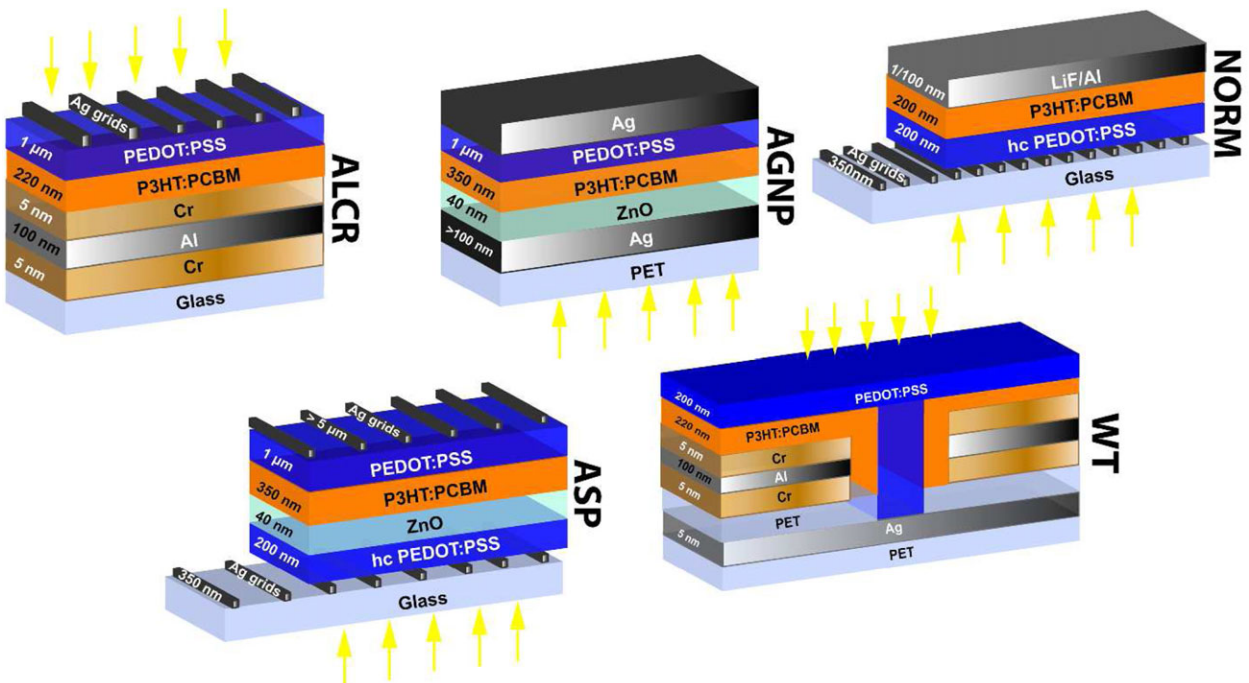

Figure 2. Schematic design of the five ITO-free architectures studied. [Color figure can be viewed in the online issue, which is available at wileyonlinelibrary.com.]

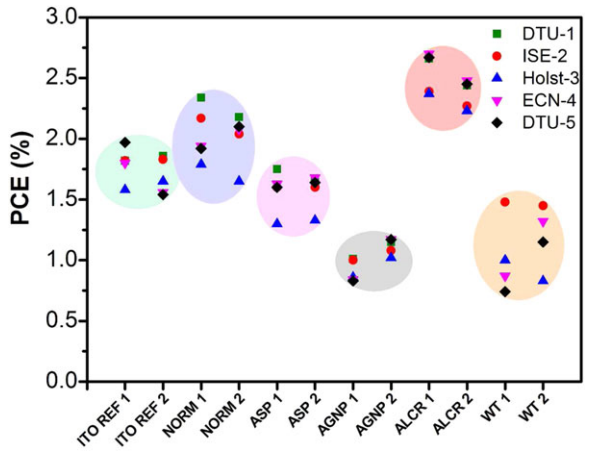

Figure 3. Round robin measurement of PCE of reference devices and ITO free architectures (two cells each) at four institutions is shown. The ovals are to help compare the deviation among the various architectures. [Color figure can be viewed in the online issue, which is available at wileyonlinelibrary.com.]

PCEs among the various architectures can be explained by the observed differences in J_{sc}, V_{oc}, and FF discussed henceforth.

The most difference among the various architectures is in J_{sc}. This can partially be explained by losses due to shading from the metal grid, absorption of the PEDOT: PSS layer which is thickness dependent, and the presence (or absence) of a reflective back electrode in any of the device. ALCR and NORM devices have metal grid and PEDOT: PSS in the path of incoming light to the photoactive polymer as well as a reflective back electrode, which explains the overall similar J_{sc} in the first measurement (DTU-1) of both ALCR and NORM devices (see Supporting Information). However, the larger standard error in the average round robin measurements of NORM devices than that established as the uncertainty (>10%) of the round robin test (previous section) signals degradation. Such degradation is not seen in ALCR devices indicating better encapsulation and more stable materials. ASP devices have slightly lower J_{sc} than either ALCR or NORM devices, which is attributed to the lack of a reflective back electrode as well as to the presence of an additional layer (ZnO) which presents two additional scattering interfaces that could lower the overall light transmission to the photoactive layer. AGNP devices have the lowest current density which is explained due to lower transmission of light (30%) through the semitransparent silver-film front electrode.[5] Absorber layer is optimized for each device structure and are all thick films (>100 nm).

Given the use of the same photoactive material, the difference in V_{oc} among the ITO-free structures could originate from several other parameters that differ among the various architectures.[10,11] Even though the most apparent difference among the various architectures is the electrodes and hence their work functions; several other factors can influence V_{oc}, for example, deposition process of the electrodes, the interfaces between the electrodes and the organic material, Fermi-level pinning and band bending, microstructure, and so forth.[11] Among the inverted devices, the most notable is the highest V_{oc} observed for ALCR devices (0.59 V) which is partly attributed to the highest electric field across the absorber polymer owing to the largest work function difference between its electrodes. The slightly lower V_{oc} for WT cells than ALCR cells is most likely attributed to parasitic resistance (shunts) due to the PEDOT: PSS channeling through the vias which also results in lower FF in WT cells. AGNP and ASP devices have similar interfaces across the photoactive region and also similar contacts which could explain the same V_{oc} observed in both architectures.

NORM devices are the only architecture in normal geometry and have lower V_{oc} than ALCR even though it has the largest work function differences across the P3HT: PCBM layer. Although one of the interfaces of the photoactive layer is formed with PEDOT: PSS in both the device architectures; however, the second interface of the photoactive layer is formed with LiF and Cr for NORM and ALCR devices respectively. According to the work function of LiF (2.5 eV) and Cr (4.0 eV), we expect higher V_{oc} for NORM than ALCR devices. When deposited in the same sequence on ITO substrates, V_{oc} of Cr based device are indeed observed to be much lower than LiF-based devices.[12] However, in our case, the opposite is seen. We attribute three reasons for this: (1) it has been observed that the work function at the interface of PEDOT: PSS/P3HT: PCBM is dependent on the sequence of deposition of PEDOT: PSS with respective to absorber layer. PEDOT: PSS deposited on top of the absorber layer has a higher work function than when deposited under the absorber layer.[13] (2) the oxidation of Cr results in Cr_2O_3: a semiconductor, which has sufficient mobility to facilitate electron transport, however, the oxidation product of Al (Al_2O_x) is an insulator. 1 nm LiF deposited on P3HT: PCBM is observed to aggregate whilst 5 nm Cr forms a more interconnected network.[12] As a result, a larger Al/absorber insulating interface is formed in case of NORM device than in the case of ALCR devices. (3) the devices were not edge-sealed and therefore, there is large possibility of oxidation of the susceptible metals. This is also the reason that the NORM devices seem to degrade even over the course of the round robin study (25 days). As a result, ALCR devices have higher V_{oc} than NORM devices and it is this parameter that leads to better PCE and stability (discussed later on) of ALCR devices than NORM devices as J_{sc} and FF of are very similar in both of these devices.

The difference in FF among the various architectures is predominantly dictated by the sheet resistance (R_{sh}) of the electrodes. In both ALCR and NORM devices, back electrode is evaporated and has a R_{sh} of <1 $\Omega\ \square^{-1}$ and the front electrode is a metal grid/PEDOT: PSS composite electrode which explains the similar FF observed for both devices. AGNP device have lower FF than ALCR devices because of the higher R_{sh} in the solution-processed silver front electrode (5 $\Omega\ \square^{-1}$) in AGNP devices. The lower FF of ASP in comparison to the NORM devices despite having similar front electrodes is explained by the difference in the back electrodes. The back electrode in ASP devices is based on PEDOT: PSS/ Ag grid where the Ag grid is screen-printed while back electrode is evaporated in NORM devices. Furthermore, the presence of two layers of PEDOT: PSS across the photoactive layer also leads to parasitic resistance, which may lead to lower FF in ASP devices. WT devices have the

Applied Polymer SCIENCE

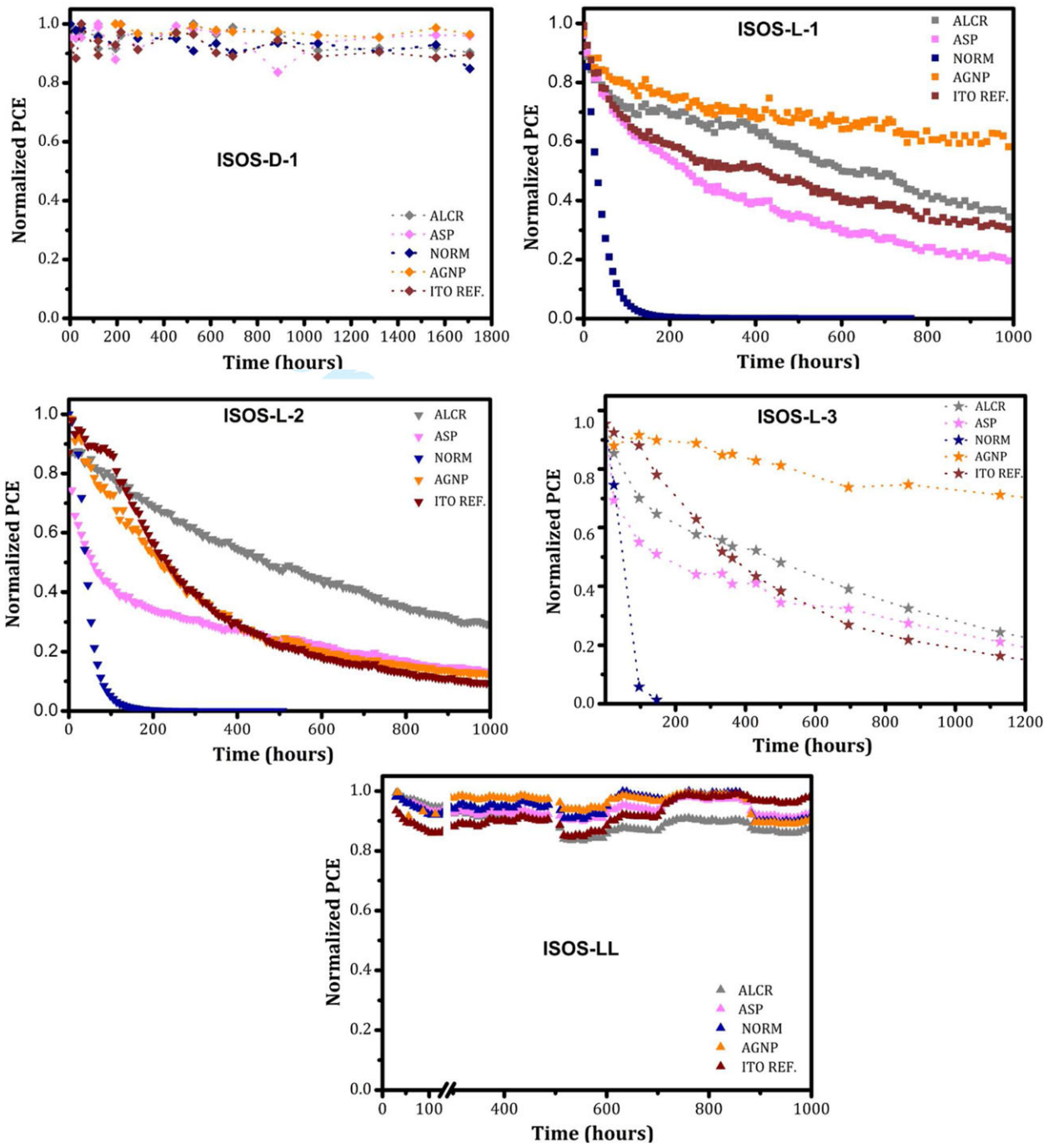

Figure 4. Stability of different architectures under ISOS-D-1 (dark/shelf life); ISOS-L-1 (1000 Wm^{-2} AM 1.5 at 37°C); ISOS-L-2 (1000 Wm^{-2} AM1.5 at 80°C); ISOS-L-3 (0.7 sun, RH 50%, 65°C); and ISOS-LL (low light at 0.1 sun, 30°C). [Color figure can be viewed in the online issue, which is available at wileyonlinelibrary.com.]

lowest FF and is attributed to additional series resistance contributed by PEDOT: PSS in the via holes as well as interfacial adherences challenges associated between the PEDOT: PSS and the via wall.[6]

Stability

Several long term degradation studies on all devices except on the WT device were carried out. Although WT devices present a very elegant and unique architecture, it was not included in the stability tests because it represented a very large uncertainty in the performance round robin (>20%), had a different active area, and also the round robin suggested a poorer stability than the other candidates in this study with a standard error of (~30%). When evaluating the stability following the many different test protocols employed, it became evident that there are large differences between the different architectures (Figure 4).

Common to all devices is that they present very good stability under ISOS-D-1 shelf life studies for 1800 h and ISOS-LL low light conditions for 1000 h and it is clear that from this point of view that all are likely to meet the criterion of compatibility with ICT applications and from this point of view upcaling efforts are warranted. When it comes to high intensity sunlight, high temperatures and humidity (ISOS-L-1/-2/-3) it is clear that the normal architecture device (NORM devices) fails quickly in all tests as expected and it is primarily attributed to the failure initiated by the oxidation of low work function Al electrode due to moisture and oxygen diffusion through the edges and the pin holes.[14–16] As the device does present stability under both shelf life and low light conditions, it is likely that this technology could be improved but the success of its use would depend on the development of efficient and low cost encapsulation methods (encapsulation with qualities beyond the method employed here) and on design improvement, for example, with the use of alternate interfacial buffer layer to LiF such as Cr,[12] C_{60}, or MoO_3[16,17] that has been shown to improve the stability by as much as a factor of 100. In its current form, upscaling of NORM devices is not warranted. The degradation patterns of the remaining three architectures and the references devices under ISOS-L-1/-2/-3 are henceforth discussed with references to degradation of J_{sc}, FF, and V_{oc}. The graphs of PCE degradation of all device architecture over time under all tests could be found in Figure 4. The graphs of degradation in FF, J_{sc}, and V_{oc} of ISOS-L1/L-2/L-3 are attached in the Supporting Information.

ISOS-L-1 test: To decipher the observed differences in the decay pattern of PCE among the various devices, one has to look at the degradation patterns in the key photovoltaic parameters, namely, J_{sc}, V_{oc}, and FF. The observed degradation trend in PCE indicates that AGNP is the most stable followed by ALCR, reference device, and ASP devices respectively. AGNP devices show no degradation in V_{oc} and FF over 1000 h but have a steady decay in J_{sc}. This decay in J_{sc} is indicative of degradation of the photoactive polymer.[16,18–24] A similar decaying trend in J_{sc} of all the devices is observed with the exception of ALCR devices that shows an increasing J_{sc} until 400 h where-after a steady decay sets in. Unlike all other devices with 1: 1 mixing ratio of P3HT: PCBM, ALCR devices contain a lower amount of PCBM (mixing ratio 1: 0.8) in the photoactive blend. At this mixing ratio, the evolution of J_{sc} suggests an annealing effect possibly causing a morphological evolution to beneficial donor: acceptor interpenetrating network as observed at the same mixing ratio reported elsewhere.[25] A similar, albeit faster evolution to peak J_{sc} (100 h) in ALCR devices at high temperature test is also observed.

Furthermore, the FF of all devices decays at a similar rate except for AGNP devices which remains constant. Such a decay in FF is attributed to degradation of PEDOT: PSS in addition to the photoactive polymer which increases resistance in the devices. The absence of edge-sealing provides an easy passage for moisture infiltration through the highly hygroscopic PEDOT: PSS layer(s) into the devices. This mechanism in addition to the transparency of the encapsulating material (glass) to UV provides a faster route to degradation in all the devices. AGNP devices, conversely, have the organic materials components sandwiched between two complete layers of Ag on both the top and the bottom of the devices, which inturn provides barrier properties. In addition, both PEDOT: PSS and photoactive polymers in AGNP devices are shielded from UV radiation because of the presence of ZnO layer that has a UV cut off at ~360 nm. These factors therefore explain the unaffected FF over 1000 h observed for AGNP devices. Conversely, the degradation of V_{oc} can directly correspond to the number of interfaces with PEDOT: PSS, particularly, the photoactive material and PEDOT: PSS is the most susceptible to degradation due to the weak adhesion between the two material layers. ASP devices have two layers of PEDOT: PSS while the reference cells have only one. Accordingly, V_{oc} of ASP devices degrades at the fastest rate followed by the reference cells. However, ALCR devices have stable V_{oc} despite the presence of PEDOT: PSS layer which leads us to believe the interfaces across the photoactive polymer is intact which is highly likely as ALCR devices are fabricated and encapsulated in N_2 environment. The loss of FF in ALCR devices therefore must originate on the exposed surface of PEDOT: PSS or the oxidation of Al/Cr contact. An indepth investigation of this is beyond the scope of this article.

ISOS-L-2: At high temperature, the degradation rate is accelerated and as such no clear trend or pattern in the degradation of J_{sc} and FF among all the devices, unlike ISOS-L-1, is observed. However, the degradation trend in V_{oc} of all the devices is similar to that observed in ISOS-L-1 test in which ALCR and AGNP devices have stable V_{oc} while the V_{oc} of all the other devices degrades, however at a faster rate than under ISOS-L-1 test.

ISOS-L-3: The relative V_{oc} degradation pattern with respect to the different device architecture in ISOS-L-3 is similar to that observed in ISOS-L-1 and ISOS-L-2, that is, ALCR and AGNP devices have stable V_{oc} over 1000 h while the other structures show decaying V_{oc}. However, the degradation pattern in J_{sc} and FF respectively of all device structure shows no clear relative trend and is because under high humidity, high temperature and sunlight, several different degradation mechanisms are in play at the same time. Nonetheless, there is a clear winner and that is AGNP devices which under ISOS-L-3 conditions remains the most stable with only 15% degradation in PCE observed after a duration 1000 h.

Architecture Selection

Based on the data described above, there is no clear winner architecture that shows high performance and high stability. The above studies can be viewed as way to reduce the number of candidates for upscaling consensually. After the degradation studies employing the five ISOS tests, the ASP, ALCR and AGNP devices still stand with the ALCR being the highest performer in terms of PCE and the AGNP architecture being the best performer with respect to overall stability. The ASP architecture can be considered an intermediate with respect to ALCR and AGNP in regard to both stability and performance. The choice among these three contenders to upscaling is not an easy one to make and will require some consideration also of the materials and processing advantages and disadvantages for each of the architectures from the point of view of upscaling via

Table IV. Comparison of the Three Architectures that were Found Most Suitable for Upscaling

Property	ASP	ALCR	AGNP
PCE	++	+++	+
	+++	++	+
Stability	+	++	+++
	+++	n.a.	n.a
Printability	+	-	-
	+	-	+
Metal free	-	-	-
	+	-	-
Vacuum free	+	-	-
	+	-	+
Ambient processing	-	-	+
	+	-	+
Flexible substrate	-	-	+
	+	+	+
Postprocessing freedom[a]	-	+	+
	-	+	+

The conclusions presented in the second row for each property are drawn from the roll-to-roll up-scaled version of each type [Drawn from Refs. 5,26, and 27].
[a]Devices with two PEDOT: PSS layers require post-processing functionalization by application of a short pulse high voltage to switch the property of one of the PEDOT: PSS layers through de-doping.[29]

facile and fast low-cost roll-to-roll (R2R) processing. Although all architectures are prototypes, several (but not all) of the materials and processing in each device architecture as employed in the prototype used in this study can be adapted for low-cost upscaling. For example, the ALCR device requires several vacuum processing steps in processing of Al/Cr and Au grid electrodes. Although Au grid can be replaced with a printable silver grid, Al/Cr has to be processed either by sputtering or evaporation or other such techniques upon upscaling where the use of vacuum is an absolute requisite. Conversely, the ASP and AGNP architectures in principle do not require vacuum processing and can both be all printed/coated. All three architectures have been upscaled[5,26–28] and in one case integrated in a demonstration application.[28] Table IV summarizes the advantages and disadvantages of all three device architectures. Plus sign (+) shows positive result and the negative sign (−) shows otherwise. For PCE and stability parameters, no negative signs are used because all devices show good photovoltaic properties with a PCE of >1% and none of the devices degrades completely (PCE to 0%) in any of the stability tests. In such a case, the relative difference among the three architecture is shown by using +++; ++; and + to indicate the best, the intermediate, and the weakest among the three architectures, respectively.

The Case for Round Robins and Interlaboratory Studies

The fundament of science is to agree on observations; and when it comes to efficiently evaluate several new ITO-free device architectures, supplied by independent laboratories, against each other; some of the most powerful tools are the round robin and/or the interlaboratory tests. Each of these tools have their own strengths and the reason for choosing one over the other is most often the practicalities linked to the topics at hand. A round robin is best suited in the evaluation of the photovoltaic performance of solar cells as one can easily compare parameters obtained for the same solar cells across several laboratories; and the execution of such a measurement takes little time and minimum resources. The results thus obtained can be used to establish the level of agreement on the photovoltaic properties of the solar cell(s) in question. If the measurements are in an agreement that is good enough to allow for comparison of the obtained values, this could justify one in taking important decisions based on them. An important decision could for instance be the choice of one device architecture out of several for further development. It can also be used to establish where a particular architecture needs to improve to qualify. The interlaboratory study is best employed where the measurement is complex and destructive making the serial process that the round robin represent impossible and where the parallel execution of such experiments would be very demanding in resources (human and instrumental) while adding little extra knowledge. The organic solar cells are an extremely complex technology where the performance achieved depends on a massive amount of parameters linked to the operator, the laboratory conditions, the process, the materials, the handling, etc. the agreement on what the performance is for a given device thus becomes impossible unless scientific groups share the materials and devices in an effort to agree vis-à-vis the brief introduction above. The use of round robins and interlaboratory studies have been reported a few times both for performance and lifetime evaluation[7–9,30–33] and have both proven powerful but they have also highlighted the current limitation in our capacity to agree on results from simple measurements of numerical data such as performance parameters of polymer solar cells. This is currently ascribed to several factors. Foremost is the need for a firm protocol which has been devised through the ISOS consensus on how to carry out and report such measurements.[1] There are however still variability, even if sought to be eliminated through the protocol, and those are linked to the operator, the solar simulators and the dynamic performance that OPV present (stability and nonlinearity). The general observation is that laboratories generally agree well on the measurement of open circuit voltage and to a certain degree fill factor, but the electrical current (J_{sc}) is often the main source of disagreement due to often large variation. This is again linked to the use of different light sources with different calibration procedures. Ideally all groups should use the same lamp that ideally should calibrate itself.[34]

CONCLUSIONS

In this work, we have presented a comparative study on various state-of-the-art ITO-free architectures contributed by various institutions. A round robin and interlaboratory methods are used to evaluate the photovoltaic properties and the stability of the architectures, respectively. Discussions on the observed differences in the photovoltaic properties and stability are presented. Based on the photovoltaic property and stability results, we have also presented a discussion on the low-cost upscaling

suitability of all architectures in their current state as proposed by the contributing institutions. Based on our experiences with R2R upscaling of several of these architectures, we have also highlighted the adoptability or lack thereof of several of the processing steps used in laboratory devices in roll-to-roll processing; and we have also have summarized the implications on the photovoltaic properties and stability when alternate processing steps are adopted as required for low-cost R2R production of these device architectures. For example, the ALCR devices present the highest photovoltaic property and reasonable stability in the laboratory cells, however, they require several processing changes in the low-cost upscaling—glove box is replaced with ambient air, evaporation of back electrode with ambient printing technique such as screen printing, evaporation of Al/Cr with sputtering, to name a few. All these factors influence the photovoltaic property and stability in the upscaled form of ALCR devices. This study highlight that when developing device architectures, one must take into account the upscaling suitability of the adopted processing technique in their development. Based on our upscaling efforts of various architectures, an all solution ambient processing like the ASP devices is the most bankable device architecture where the photovoltaic properties of the upscaled devices processed through ambient air R2R processing is most likely to be closer to the performance of the laboratory cells as drastic processing changes are not required when going from laboratory scale to R2R. Finally, we have shown that an architecture that presents a high score in only one aspect of solar cell performance is not sufficient to justify an investment in upscaling. Many will require further technical development.

ACKNOWLEDGMENTS

This work has been supported by the European Commission as part of Framework 7 ICT 2009 collaborative project HIFLEX (Grant no. 248678). We thank Suren Gevorgyan and Thue T. Larsen-Olsen for carrying out few measurements.

REFERENCES

1. Reese, M. O.; Gevorgyan, S. A.; Jørgensen, M.; Bundgaard, E.; Kurtz, S. R.; Ginley, D. S.; Olson, D. C.; Lloyd, M. T.; Morvillo, P.; Katz, E. A.; Elschner, A.; Haillant, O.; Currier, T. R.; Shrotriya, V.; Hermenau, M.; Riede, M.; R. Kirov, K.; Trimmel, G.; Rath, T.; Inganäs, O.; Zhang, F.; Andersson, M.; Tvingstedt, K.; Lira-Cantu, M.; Laird, D.; McGuiness, C.; Gowrisanker, S. (.; Pannone, M.; Xiao, M.; Hauch, J.; Steim, R.; DeLongchamp, D. M.; Rösch, R.; Hoppe, H.; Espinosa, N.; Urbina, A.; Yaman-Uzunoglu, G.; Bonekamp, J.; van Breemen, A. J. J. M.; Girotto, C.; Voroshazi, E.; Krebs, F. C. *Solar Energy Mater. Solar Cells* **2011**, *95*, 1253.
2. Galagan, Y.; Zimmermann, B.; Coenen, E. W. C.; Jørgensen, M.; Tanenbaum, D. M.; Krebs, F. C.; Gorter, H.; Sabik, S.; Slooff, L. H.; Veenstra, S. C.; Kroon, J. M.; Andriessen, R. *Adv. Energy Mater.* **2012**, *2*, 103.
3. Galagan, Y.; Coenen, E. W. C.; Sabik, S.; Gorter, H. H.; Barink, M.; Veenstra, S. C.; Kroon, J. M.; Andriessen, R.; Blom, P. W. M. *Solar Energy Mater. Solar Cells* **2012**, *104*, 32.
4. Zimmermann, B.; Würfel, U.; Niggemann, M. *Solar Energy Mater. Solar Cells* **2009**, *93*, 491.
5. Angmo, D.; Hösel, M.; Krebs, F. C. *Solar Energy Mater. Solar Cells* **2012**, *107*, 329.
6. Zimmermann, B.; Glatthaar, M.; Niggemann, M.; Riede, M. K.; Hinsch, A.; Gombert, A. *Solar Energy Mater. Solar Cells* **2007**, *91*, 374.
7. Larsen-Olsen, T. T.; Machui, F.; Lechene, B.; Berny, S.; Angmo, D.; Søndergaard, R.; Blouin, N.; Mitchell, W.; Tierney, S.; Cull, T.; Tiwana, P.; Meyer, F.; Carrasco-Orozco, M.; Scheel, A.; Lövenich, W.; de Bettignies, R.; Brabec, C. J.; Krebs, F. C. *Adv. Energy Mater.* **2012**, *2*, 1091.
8. Gevorgyan, S. A.; Medford, A. J.; Bundgaard, E.; Sapkota, S. B.; Schleiermacher, H.; Zimmermann, B.; Wuerfel, U.; Chafiq, A.; Lira-Cantu, M.; Swonke, T.; Wagner, M.; Brabec, C. J.; Haillant, O. O.; Voroshazi, E.; Aernouts, T.; Steim, R.; Hauch, J. A.; Elschner, A.; Pannone, M.; Xiao, M.; Langzettel, A.; Laird, D.; Lloyd, M. T.; Rath, T.; Maier, E.; Trimmel, G.; Hermenau, M.; Menke, T.; Leo, K.; Roesch, R.; Seeland, M.; Hoppe, H.; Nagle, T. J.; Burke, K. B.; Fell, C. J.; Vak, D.; Singh, T. B.; Watkins, S. E.; Galagan, Y.; Manor, A.; Katz, E. A.; Kim, T.; Kim, K.; Sommeling, P. M.; Verhees, W. J. H.; Veenstra, S. C.; Riede, M.; Christoforo, M. G.; Currier, T.; Shrotriya, V.; Schwartz, G.; Krebs, F. C. *Solar Energy Mater. Solar Cells* **2011**, *95*, 1398.
9. Krebs, F. C.; Gevorgyan, S. A.; Gholamkhass, B.; Holdcroft, S.; Schlenker, C.; Thompson, M. E.; Thompson, B. C.; Olson, D.; Ginley, D. S.; Shaheen, S. E.; Alshareef, H. N.; Murphy, J. W.; Youngblood, W. J.; Heston, N. C.; Reynolds, J. R.; Jia, S.; Laird, D.; Tuladhar, S. M.; Dane, J. G. A.; Atienzar, P.; Nelson, J.; Kroon, J. M.; Wienk, M. M.; Janssen, R. A. J.; Tvingstedt, K.; Zhang, F.; Andersson, M.; Inganäs, O.; Lira-Cantu, M.; de Bettignies, R.; Guillerez, S.; Aernouts, T.; Cheyns, D.; Lutsen, L.; Zimmermann, B.; Würfel, U.; Niggemann, M.; Schleiermacher, H.; Liska, P.; Grätzel, M.; Lianos, P.; Katz, E. A.; Lohwasser, W.; Jannon, B. *Solar Energy Mater. Solar Cells* **2009**, *93*, 1968.
10. Scharber, M. C.; Mühlbacher, D.; Koppe, M.; Denk, P.; Waldauf, C.; Heeger, A. J.; Brabec, C. C. *Adv Mater* **2006**, *18*, 789.
11. Qi, B.; Wang, J. *J. Mater. Chem.* **2012**, *22*, 24315.
12. Wang, M.; Tang, Q.; An, J.; Xie, F.; Chen, J.; Zheng, S.; Wong, K. Y.; Miao, Q.; Xu, J. *ACS Appl. Mater. Interfaces* **2010**, *2*, 2699.
13. Glatthaar, M.; Niggemann, M.; Zimmermann, B.; Lewer, P.; Riede, M.; Hinsch, A.; Luther, J. *Thin Solid Films* **2005**, *491*, 298.
14. Lloyd, M. T.; Olson, D. C.; Lu, P.; Fang, E.; Moore, D. L.; White, M. S.; Reese, M. O.; Ginley, D. S.; Hsu, J. W. P. *J. Mater. Chem.* **2009**, *19*, 7638.
15. Norrman, K.; Gevorgyan, S. A.; Krebs, F. C. *ACS Appl. Mater. Interfaces* **2009**, *1*, 102.
16. Voroshazi, E.; Verreet, B.; Buri, A.; Müller, R.; Di Nuzzo, D.; Heremans, P. *Org. Electron.* **2011**, *12*, 736.
17. Yamanari, T.; Taima, T.; Sakai, J.; Tsukamoto, J.; Yoshida, Y. *Jpn J. Appl. Phys.* **2010**, *49*, 01AC02.

18. Voroshazi, E.; Verreet, B.; Aernouts, T.; Heremans, P. *Solar Energy Mater. Solar Cells* **2011**, *95*, 1303.

19. Rivaton, A.; Chambon, S.; Manceau, M.; Gardette, J.; Lemaître, N.; Guillerez, S. *Polym. Degrad. Stab.* **2010**, *95*, 278.

20. Manceau, M.; Rivaton, A.; Gardette, J.; Guillerez, S.; Lemaître, N. *Polym. Degrad. Stab.* **2009**, *94*, 898.

21. Schafferhans, J.; Baumann, A.; Wagenpfahl, A.; Deibel, C.; Dyakonov, V. *Org. Electron. Phys. Mater. Appl.* **2010**, *11*, 1693.

22. Seemann, A.; Egelhaaf, H.; Brabec, C. J.; Hauch, J. A. *Org. Electron. Phys. Mater. Appl.* **2009**, *10*, 1424.

23. Liao, H..; Yang, C.; Liu, C.; Horng, S.; Meng, H.; Shy, J. *J. Appl. Phys.* **2008**, *103*, 104506.

24. Reese, M. O.; Nardes, A. M.; Rupert, B. L.; Larsen, R. E.; Olson, D. C.; Lloyd, M. T.; Shaheen, S. E.; Ginley, D. S.; Rumbles, G.; Kopidakis, N. *Adv. Funct. Mater.* **2010**, *20*, 3476.

25. Ma, W.; Yang, C.; Gong, X.; Lee, K.; Heeger, A. *Adv. Funct. Mater.* **2005**, *15*, 1617.

26. Manceau, M.; Angmo, D.; Jørgensen, M.; Krebs, F. C. *Org. Electron. Phys. Mater. Appl.* **2011**, *12*, 566.

27. Angmo, D.; Gevorgyan, S. A.; Larsen-Olsen, T. T.; Søndergaard, R.; Hösel, M.; Jørgensen, M.; Gupta, R.; Kulkarni, G. U.; Krebs, F. C. *Org. Electron.* **2013**, *14*, 984.

28. Angmo, D.; Larsen-Olsen, T. T.; Jørgensen, M.; Søndergaard, R. R.; Krebs, F. C. *Adv. Energy Mater.* **2012**; doi: 10.1002/aenm.201200520.

29. Larsen-Olsen, T.T.; Søndergaard, R.R; Norrman, K.; Jørgensen, M.; Krebs, F.C. *Energy Environ. Sci.* **2012**, *5*, 9467.

30. Andreasen, B.; Tanenbaum, D. M.; Hermenau, M.; Voroshazi, E.; Lloyd, M. T.; Galagan, Y.; Zimmernann, B.; Kudret, S.; Maes, W.; Lutsen, L.; Vanderzande, D.; Wuerfel, U.; Andriessen, R.; Roesch, R.; Hoppe, H.; Teran-Escobar, G.; Lira-Cantu, M.; Rivaton, A.; Uzunoglu, G. Y.; Germack, D. S.; Hösel, M.; Dam, H. F.; Jørgensen, M.; Gevorgyan, S. A.; Madsen, M. V.; Bundgaard, E.; Krebs, F. C.; Norrman, K. *Phys. Chem. Chem. Phys.* **2012**, *14*, 11870.

31. Tanenbaum, D. M.; Hermenau, M.; Voroshazi, E.; Lloyd, M. T.; Galagan, Y.; Zimmermann, B.; Hösel, M.; Dam, H. F.; Jørgensen, M.; Gevorgyan, S. A.; Kudret, S.; Maes, W.; Lutsen, L.; Vanderzande, D.; Wuerfel, U.; Andriessen, R.; Roesch, R.; Hoppe, H.; Teran-Escobar, G.; Lira-Cantu, M.; Rivaton, A.; Uzunoglu, G. Y.; Germack, D.; Andreasen, B.; Madsen, M. V.; Norrman, K.; Krebs, F. C. *RSC Adv.* **2012**, *2*, 882.

32. Roesch, R.; Tanenbaum, D. M.; Jørgensen, M.; Seeland, M.; Baerenklau, M.; Hermenau, M.; Voroshazi, E.; Lloyd, M. T.; Galagan, Y.; Zimmermann, B.; Wuerfel, U.; Hoesel, M.; Dam, H. F.; Gevorgyan, S. A.; Kudret, S.; Maes, W.; Lutsen, L.; Vanderzande, D.; Andriessen, R.; Teran-Escobar, G.; Lira-Cantu, M.; Rivaton, A.; Uzunoglu, G. Y.; Germack, D.; Andreasen, B.; Madsen, M. V.; Norrman, K.; Hoppe, H.; Krebs, F. C. *Energy Environ. Sci.* **2012**, *5*, 6521.

33. Teran-Escobar, G.; Tanenbaum, D. M.; Voroshazi, E.; Hermenau, M.; Norrman, K.; Lloyd, M. T.; Galagan, Y.; Zimmermann, B.; Hösel, M.; Dam, H. F.; Jørgensen, M.; Gevorgyan, S.; Kudret, S.; Maes, W.; Lutsen, L.; Vanderzande, D.; Wuerfel, U.; Andriessen, R.; Roesch, R.; Hoppe, H.; Rivaton, A.; Uzunoglu, G. Y.; Germack, D.; Andreasen, B.; Madsen, M. V.; Bundgaard, E.; Krebs, F. C.; Lira-Cantu, M. *Phys. Chem. Chem. Phys.* **2012**, *14*, 11824.

34. Krebs, F. C.; Sylvester-Hvid, K. O.; Jørgensen, M. *Prog. Photovoltaics Res. Appl.* **2011**, *19*, 97.